Inorganic Chemistry

ARTICLE

pubs.acs.org/IC

Synthesis and Antiproliferative Activity of a C,N-Cycloplatinated(II) Complex with a Potentially Intercalative Anthraquinone Pendant

José Ruiz,*[,†] Consuelo Vicente,[†] Concepción de Haro,[†] and Arturo Espinosa[‡]

[†]Departamento de Química Inorgánica, Universidad de Murcia, 30071- Murcia, Spain

[‡]Departamento de Química Orgánica, Universidad de Murcia, 30071- Murcia, Spain

ABSTRACT: The synthesis of the novel anthraquinone platinum derivate [Pt(ppy)Cl(1C3)] (**2**) [Hppy = N,C-chelating 2-phenylpyridine; 1C3 = 1-[(3-aminopropyl)amino]-anthracene-9,10-dione] and its values of IC_{50} against a panel of human tumor cell lines representative of ovarian (A2780 and A2780*cis*R) and breast cancers (T47D) are reported. At 24 h incubation time, complex **2** was more active than cisplatin (about 9-fold) and the free ligand 1C3 (about 2-fold) in T47-D. The observation that the cisplatin IC_{50} falls by about 10-fold from 24 to 72 h, whereas that for **2** changes little, suggests substantial differences in the mode of action. Complex **2** also showed high cytotoxicity against A2780 (about 3-fold greater than cisplatin at 24 h). On the other hand, very low resistance factors (RF) of **2** in A2780*cis*R at 24−72 h (RF = 1.3) were observed. The interaction of **2** with DNA was followed by electrophoretic mobility and UV−visible spectroscopy, and its reaction with the model nucleobase 9-EtG was studied by ^{1}H NMR and ESI-MS. Theoretical calculations at the B3LYP/def2-TZVPP//BP86/def2-TZVP level of theory on complex **2** show a labile Pt−Cl bond that allows easy replacement of Cl by *N*-nucleophiles such as 9-EtG, which forms a stronger Pt−N bond.

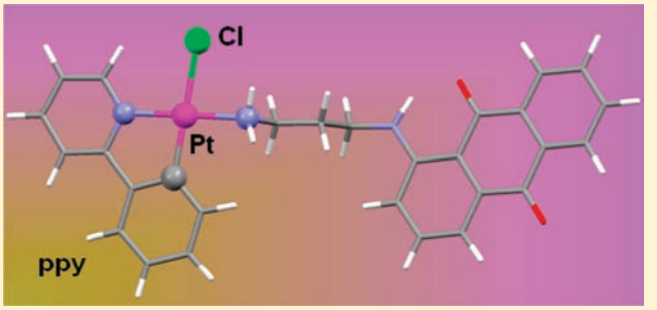

INTRODUCTION

Platinum-based compounds are widely used in antitumor therapy of solid tumors and represent the cornerstone for the treatment of testicular and ovarian tumors and lung and colorectal carcinomas.[1−5] Despite the therapeutic benefit of platinum-based treatment regiments, the efficacy of platinum drugs is still limited by side effects and intrinsic and acquired resistances.[6−8] In order to increase the rate and extent of localization of the platinum in the vicinity of its target, DNA, thereby decreasing the number of side reactions on route to the target and to increase the rate of reaction with the nucleobases, a number of investigators have prepared and investigated platinum complexes with DNA intercalators attached.[9−23] Alkylamino-anthraquinone containing compounds such as the anthracycline antibiotic doxorubicin are established and clinically used anticancer drugs (trade name adriamyacin, Scheme 1a). Doxorubicin and other related anthraquinones, such as 1C3 [(**1**), 1C3 = 1-[(3-aminopropyl)amino]-anthracene-9,10-dione, Scheme 1b], are known to intercalate into DNA; and hence, a Pt-anthraquinone pendant derivative may represent an effective system for the delivery of the platinum moiety to nuclear DNA. The synthesis of several aminoalkylamino anthraquinones platinum complexes[14−23] has been reported, and the cellular distribution of the antraquinone derivative **1** and the platinum-anthraquinone hybrids *cis*-[$PtCl_2$(1C3)(NH_3)] and [Pt(1C3)(dien)]$^{2+}$ (dien = 3-azapentane-1,5-diamine) has been recently investigated by Hambley and coworkers.[24,25]

In this context, we have recently reported the preparation of some new *C,N*-cycloplatinated(II) complexes that display high cytotoxicity against the human acute promyelocytic leukemia cell line HL-60[26] and breast cancers (T47D).[27,28]

In order to increase the selectivity and hydrophobicity of cycloplatinated derivatives, we report herein the synthesis and characterization of the novel platinum derivative [Pt(ppy)Cl-(1C3)] (Hppy = N,C-chelating 2-phenylpyridine), which could be able to interact with DNA through both intercalative and coordinative binding modes. Values of IC_{50} were studied for the new platinum complex against a panel of human tumor cell lines representative of ovarian (A2780 and A2780*cis*R), and breast cancers (T47D, cisplatin resistant). The interaction of the new platinum complex with DNA has also been studied.

RESULTS AND DISCUSSION

Synthesis of the Cycloplatinated(II) Complex [Pt(ppy)Cl(1C3)] 2. The ready reaction of [Pt(ppy)(μ-Cl)]$_2$ in $CHCl_3$ with 1C3 in a 1:2 molar ratio gives the mononuclear complex **2** (Scheme 2).

The resulting red complex is air-stable, both in the solid state and in solution and was characterized by ^{1}H, ^{13}C, and ^{195}Pt NMR spectroscopy, positive-ion ESI-MS, and IR spectroscopy and gave satisfactory elemental analyses. The far-IR **2** exhibits a band

Received: July 29, 2010
Published: February 11, 2011

dx.doi.org/10.1021/ic101526h | *Inorg. Chem.* 2011, 50, 2151–2158

Scheme 1. 1C3 [(1), 1C3 = 1-[(3-aminopropyl)amino]-anthracene-9,10-dione

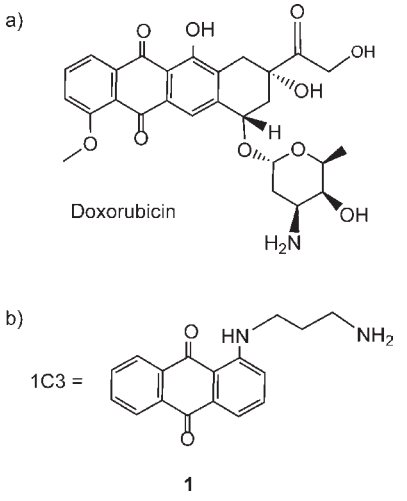

Scheme 2. Cycloplatinated(II) Complex [Pt(ppy)Cl(1C3)]

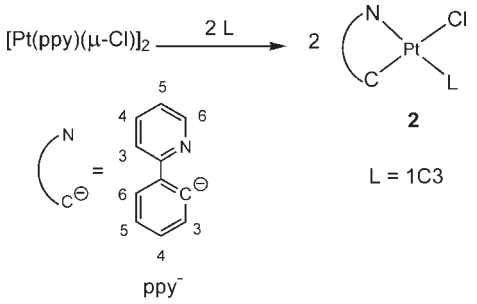

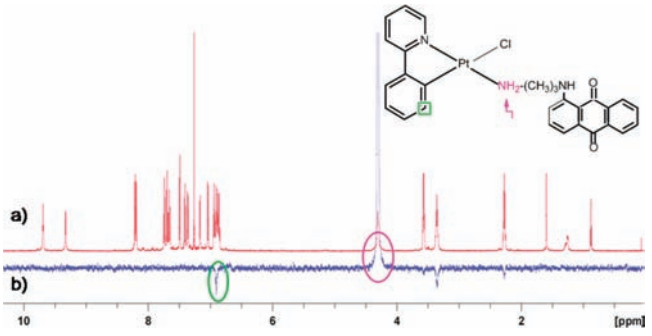

Figure 1. (a) ^{1}H NMR spectrum of complex **2** in $CDCl_3$ at room temperature. (b) NOE difference spectrum (mixing time: 0.8 s) with signal irradiation at 4.37 ppm.

assigned to ν(Pt−Cl) at 227 cm^{-1}. All signals in the ^{1}H NMR spectrum of complex **2** (Figure 1a) were unequivocally assigned by 2D and NOE techniques. ^{195}Pt satellites are observed as shoulders for the H6 (of the pyridyl ring) signal. In the 1D-NOE difference spectrum (Figure 1b), the strong NOE observed between the NH_2 protons and the aromatic H3 resonance of the phenyl group in the bidentate ppy ligand indicates the proximity of the referred nuclei. The selective irradiation at

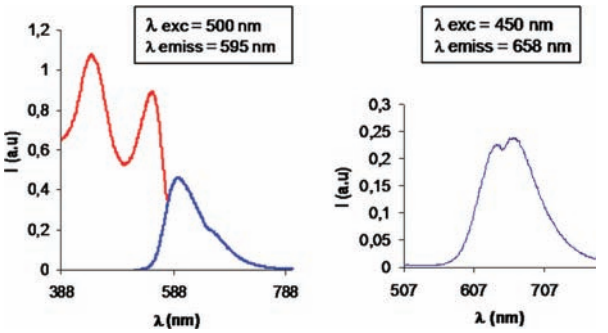

Figure 2. Excitation (red) and emission (blue) spectra for complex **2** in 5×10^{-4} M CH_2Cl_2 solution at room temperature (left). Emission spectra for complex **2** in the solid state at room temperature (right).

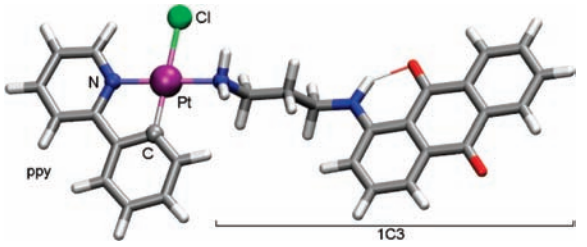

Figure 3. Calculated structure for **2**.

δ 4.37 ppm produced a clear NOE enhancement at the aromatic signal at δ 6.92 ppm (green ellipse in Figure 1b) that supports the location of the amino group close (*cis*) to the phenyl ppy ring, in agreement with the ^{1}H^{1}and H−COSY results.

Complex **2** is fluorescent in the solid state at room temperature, displaying (Figure 2) a structured emission at 658 nm (λ exc. 450 nm) that is similar to that displayed by the free 1C3 ligand.

Theoretical Calculations on Complex 2. Some insight into the structural and reactivity features of complex **2** was obtained with the aid of quantum chemical calculations. The structure corresponding to the absolute minimum in the potential energy surface at the BP86/def2-TZVP level of theory (see Computational Details) displays a fully extended conformation (Figure 3, generated with VMD) with the external flat moieties roughly parallel. The Pt atom is located in an almost regular square−plannar environment (dihedral N_{ppy}−C_{ppy}−N_{1C3}−Cl 0.3°) formed by two nitrogen, one carbon, and one chlorine donor atoms (Do). Assessment of Pt−Do bond strengths has been achieved within the framework of Bader's atoms-in-molecules (AIM) theory[29] by computing the electron density at the respective bond critical points (BCP). According to this criterion, the three strongest bonds to platinum are formed by the ppy C-atoms (d_{Pt-C} = 1.992 Å; $\rho(\mathbf{r}_c)$ = 15.76 × 10^{-2} e/a_o^3) and N-atoms (d_{Pt-N} = 2.017 Å; $\rho(\mathbf{r}_c)$ = 12.87 × 10^{-2} e/a_o^3), as well as the 1C3 N-atom (d_{Pt-N} = 2.080 Å; $\rho(\mathbf{r}_c)$ = 11.19 × 10^{-2} e/a_o^3), whereas the bond to Cl ligand (d_{Pt-Cl} = 2.420 Å; $\rho(\mathbf{r}_c)$ = 7.78 × 10^{-2} e/a_o^3) is considerably weaker. Indeed, the latter is the only ligand around Pt bearing a large negative charge (q^N = −0.575 au) in contrast to the remarkable low value of the other formally anionic ligand ppy (q^N = −0.123 au) and the positive charge at the 1C3 moiety (q^N = 0.294 au). These facts agree with the observed reactivity toward N-nucleophiles (see below) undergoing fast chloride substitution at Pt. An additional feature that contributes to the plannarity of Do atoms around Pt is the existence of a secondary interaction between the Cl ligand and the closest ppy

dx.doi.org/10.1021/ic101526h |*Inorg. Chem.* 2011, 50, 2151–2158

Table 1. $IC_{50}(\mu M)$ and Resistance Factors for Cisplatin and Compounds 1 and 2

	T47D			A2780			A2780*cis*R (RF)[a]			LLC-PK1
compound	24 h	48 h	72 h	24 h	48 h	72 h	24 h	48 h	72 h	48 h
1	42 ± 1	30 ± 1	26 ± 1	27 ± 1	19 ± 1	14 ± 1	19 ± 1 (0.7)	20 ± 3 (1.1)	22 ± 1 (1.6)	--
2	21 ± 1	17 ± 3	13 ± 1	7.2 ± 0.2	7.8 ± 0.2	8.0 ± 0.2	9.6 ± 0.2 (1.3)	9.8 ± 0.2 (1.3)	10 ± 1 (1.3)	18 ± 1
cisplatin	190 ± 12	59 ± 5	16 ± 1	18 ± 1	3.0 ± 0.1	1.7 ± 0.2	34 ± 1 (1.9)	14 ± 2 (4.7)	8.0 ± 0.3 (4.8)	9.5 ± 0.9

[a] The numbers in parentheses are the resistance factors (RF) (IC_{50} resistant/IC_{50} sensitive).

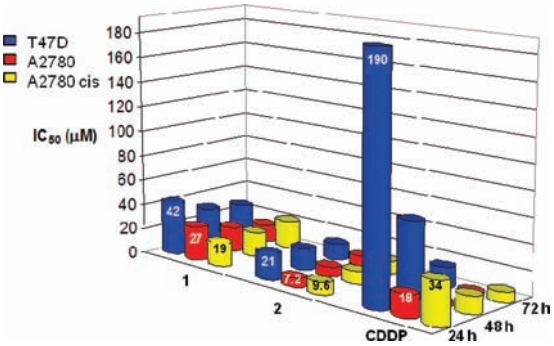

Figure 4. Toxicity of **1**, **2**, and cisplatin (IC_{50} μM) in ovarian and breast cell lines. Effect of cisplatin resistance.

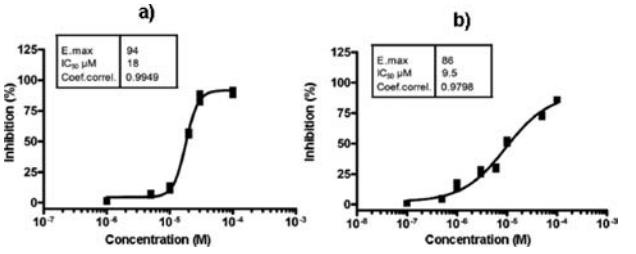

Figure 5. Curves of inhibition of cellular growth in the normal LLC-PK1 renal cells after 48 h incubated with complex **2** (a) and cisplatin (b).

H atom ($d_{Cl\cdots H}$ = 2.575 Å; $\rho(\mathbf{r}_c)$ = 1.34 × 10^{-2} e/a_o^3). An even weaker interaction is observed between a ppy H atom on the other (phenyl) ring and a 1C3 NH atom ($d_{ppyH\cdots HN}$ = 2.283 Å; $\rho(\mathbf{r}_c)$ = 0.70 × 10^{-2} e/a_o^3), this contact being responsible for the aforementioned positive NOE (Figure 1).

Biological Activity: Cytotoxicity Studies. To analyze the potential of **2** as an antitumor agent, its cytotoxicity was measured (at 24, 48, and 72 h; Table 1 and Figure 4) toward the human breast cancer (T47D, cisplatin resistant) and epithelial ovarian carcinoma cells A2780 and A2780*cis*R (acquired resistance to cisplatin), and for comparison purposes, the cytotoxicity of cisplatin and the free ligand **1** was also evaluated under the same experimental conditions. Because of low aqueous solubility, the test compounds were dissolved in DMSO first and then serially diluted in complete culture medium such that the effective DMSO content did not exceed 1%. It is noteworthy that at 24 h incubation time the T47-D complex **2** was more active than cisplatin (about 9-fold) and the free ligand **1** (about 2-fold). The observation that cisplatin IC_{50} falls by about 10-fold from 24 to 72 h, whereas that for **2** changes little, suggests substantial differences in the mode of action. Complex **2** also showed high cytotoxicity against an A2780 cancer cell line (about 3-fold greater than that of cisplatin at 24 h). On the other hand, A2780*cis*R encompasses all of the known major mechanisms of resistance to cisplatin: reduced drug transport,[30] enhanced DNA repair/tolerance,[31] and elevated GSH levels.[32] The ability of complex **2** to circumvent cisplatin acquired resistance was determined from the resistance factor (RF), defined as the ratio of IC_{50} resistant line to IC_{50} parent line. An RF of <2 was considered to denote noncross-resistance.[33] Very low resistance factors (RF) of **2** at 24−72 h (RF = 1.3) were observed. In vitro antiproliferative activity of complex **2** and cisplatin was also evaluated in normal human LLC-PK1 renal cells at 48 h (Table 1). As shown in Table 1 at 9.8 μM, after 48 h, complex **2** is able to kill half of the A2780*cis*R cells and only about 10% of LLC-PK1 renal cells (Figure 5a). At the same concentration cisplatin is able to kill less than half of the A2780*cis*R cells and about half of the normal LLC-PK1 renal cells (Figure 5b).

On the other hand, the stability of the cytotoxic compound **2** has been tested in DMSO-d_6 by ^{1}H NMR, remaining unaltered after three days in solution at room temperature. As expected, complex **2** in DMSO-d_6/D_2O (1:1 in volume), at 37 °C, undergoes a fast (and complicated) hydrolisis process; a reaction that can be reversed by addition of sodium chloride (1:100 molar ratio).

Platinum Cellular Accumulation Studies. We have determined the Pt accumulation in T47D cell line after 24, 48, and 72 h continuous exposure with 20 μM of complex **2** and cisplatin (Table 2 and Figure 6). A direct relationship between Pt accumulation and activity has not been described yet, and it is not clearly observed in our measurements[34,35] because cisplatin is the complex with greater uptake at 24 h but is not the metal complex with the highest cytotoxicity at this time.

Compound **2** exhibits a better capacity than cisplatin to reach the cell at 48 and 72 h (∼1.6 and 3 times, respectively).

Biological Assays: Gel Electrophoresis of Compound−pB*R*322 Complexes. The DNA binding of compounds **1** and **2** was compared by reacting them with pB*R*322 plasmid DNA at at 37 °C for 24 h and separating the products using gel electrophoresis. Both compounds are able to modify the electrophoretic mobility of the covalently closed circular (ccc) and open (oc) forms of plasmid DNA (Figure 7). The anthraquinone derivative **1** by itself produces very little change in the mobility or unwinding of the supercoiled DNA (Figure 7a) probably because of the high lability of the intercalation of the simple anthraquinones preventing any permanent unwinding of the DNA.[36] In contrast, when the pB*R*322 was incubated with the platinum compound **2**, at r_i = 0.48, a single band for both forms, ccc and oc, and the coalescent form was observed (Figure 7b). A similar pattern has been found previously in some others C,N-cycloplatinated complexes.[28]

UV-Spectrophotometric Titrations. UV-spectrophotometric titrations were carried out to determine the affinity of the platinum complex **2** for DNA. Salmon sperm DNA (0−300 μM) was added in aliquots to a solution of **2** (27 μM), and the UV-spectra were recorded (Figure 8a). Using the absorbance

dx.doi.org/10.1021/ic101526h |*Inorg. Chem.* 2011, 50, 2151–2158

Table 2. Cellular Platinum Concentrations in Human Breast Carcinoma T47D Cells[a]

compound	cellular uptake[a] (pmol Pt/10^6 cells) 24 h	cellular uptake[a] (pmol Pt/10^6 cells) 48 h	cellular uptake[a] (pmol Pt/10^6 cells) 72 h
2	3.964 ± 0.006	3.608 ± 0.007	2.365 ± 0.003
cisplatin	4.388 ± 0.005	2.231 ± 0.005	0.778 ± 0.001

[a] Drug-treatment period with 20 μM Pt complexes. Each value represents the mean ± SD of three determinations from two independent experiments. Cisplatin in whole cells. Results are the mean ± SD of three determinations from two independent experiments.

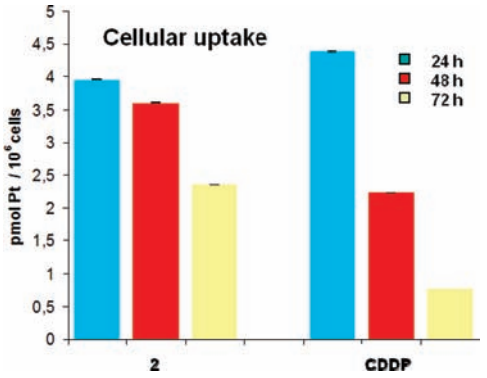

Figure 6. Platinum concentrations determined in T47D cells after 24, 48, and 72 h of exposure to 20 μM complex **2** and cisplatin in whole cells. Results are the mean ± SD of three determinations from two independent experiments.

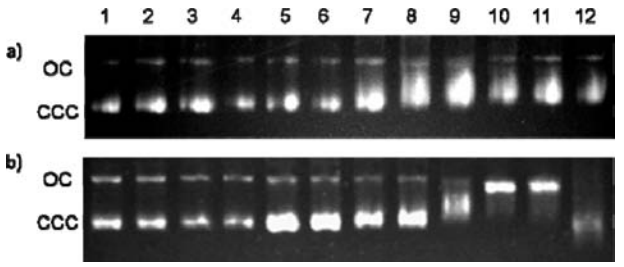

Figure 7. Electrophoretic mobility pattern of pBR322 plasmid DNA incubated with the compounds **1** (a) and **2** (b). The lanes (from left to right) correspond to control-DNA only, then concentrations of 0.097, 0.195, 0.390, 0.780, 1.600, 3.125, 6.25, 12.5, 25, 50, and 100 μM of compound **1** or **2** incubated with DNA.

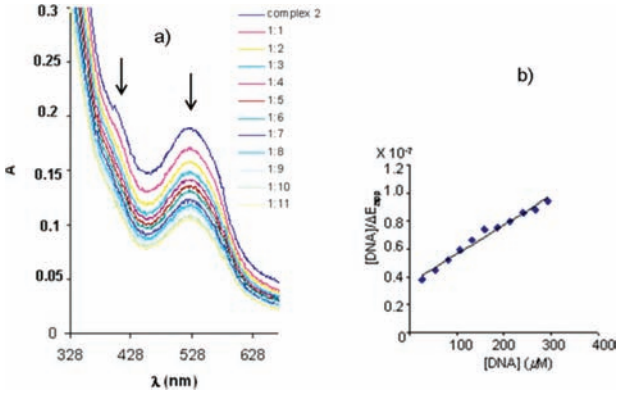

Figure 8. (a) UV-spectrophotometric titration curves and (b) half reciprocal plot obtained from titrating **2** (27 μM) with salmon sperm DNA in a 1:1 to 1:11 ratio.

values where the greatest change in the spectrum was observed, half reciprocal plots were generated (Figure 8b) and used as previously

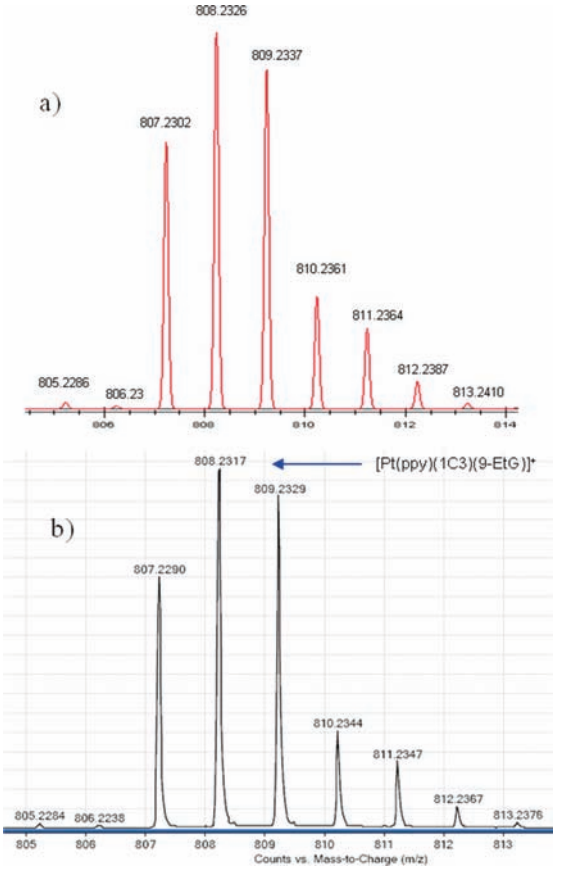

Figure 9. (a) Theoretical ESI mass spectrum of 3^+. (b) Experimental ESI mass spectrum of the reaction of complex **2** with 9-ethylguanine after 15 min at 37 °C.

described.[36,37] The binding constant of **2** was found to be 5×10^3 M^{-1} (the uncomplexed anthraquinone **1**, 1C3, has[23] an apparent DNA binding constant of 1.4×10^4, similar to that of ethidium bromide). The addition of DNA to each of the compounds resulted in a bathochromic shift of 4−8 nm, and no isosbestic points were observed in the titrations. The absorbance was measured at 502 nm for complex **2**. At this wavelength, the absorbance intensity was seen to steadily decrease with increasing DNA concentration (hypochromism of about 30%), which is indicative of π-stacking interactions.[18,37]

Reaction of the Platinum Complex 2 with 9-Ethylguanine. To gain further insight into the mechanism of the interaction of the new platinum complex with DNA, the reaction of **2** with an excess of 9-ethylguanine, as a model nucleobase, was carried out in ^{1}H NMR at physiological temperature and pH. According to the expected reactivity as previously derived from the DFT calculations on **2**, the reaction is fast, and in less than 15 min the formation of the complex $[Pt(ppy)(1C3)(9\text{-EtG})]^+$ (3^+) is completed. No more changes were observed after 3 days. The signal for the H(8) of

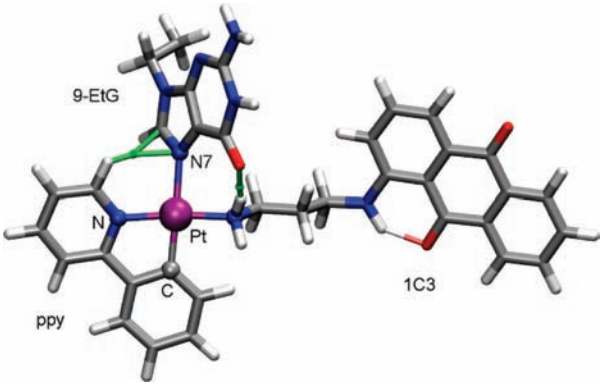

Figure 10. Calculated structure for adduct 3^+. Small green spheres represent BCP for secondary interactions involving the 9-EtG ligand.

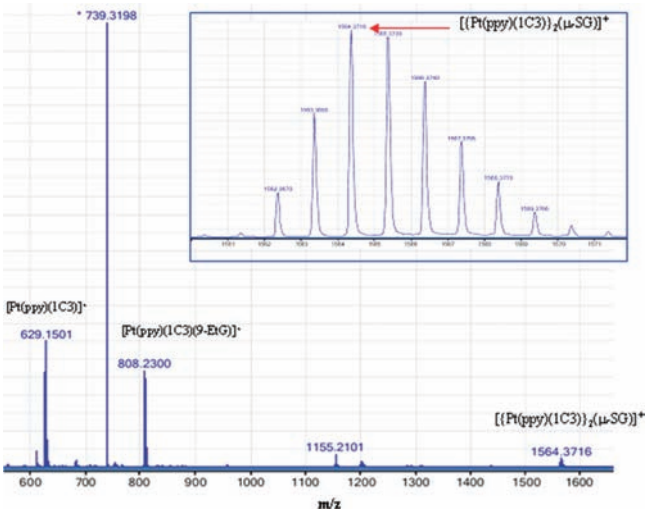

Figure 11. Experimental ESI mass spectrum of the reaction of complex **2** with 9-ethylguanine and glutathione after 24 h. Inset: Expanded spectrum highlighting the dinuclear complex 4^+.

the free guanine moves downfield upon coordination, and the ratio coordinated H8 of 9-EtG/aromatics H of ppy agrees well with the formation of the monoadduct with 9-EtG.

Further evidence of the formation of the $[Pt(ppy)(1C3)(9\text{-EtG})]^+$ derivative comes from ESI-MS analysis of the reaction mixtures, a peak in the mass spectra corresponding to a signal assignable to the 9-EtG platinum monoadduct being observed (Figure 9).

The calculated structure for the substitution product 3^+ shows the 9-EtG moiety coordinated to the metal through its basic N7 atom (Figure 10). According to our calculations, the strength of the not involved Pt−Do bonds is kept roughly unchanged,[38] whereas the newly formed Pt−N bond ($d_{Pt-N} = 2.195$ Å; $\rho(\mathbf{r}_c) = 8.22 \times 10^{-2}$ e/a_o^3) is significantly weaker than the other Pt-ligand interactions and barely stronger—and hence more stable—than the substituted Pt−Cl one. These Pt−Do bond differences by themselves are too small to account for the observed stability of the adduct 3^+, and a set of secondary interactions observed in the gas-phase structure far away from the platinum coordination sphere[39] should play a decisive role and could be extrapolated to the actual binding of **2** to DNA.

Reaction of the Platinum Complex 2 with 9-Ethylguanine in the Presence of Glutathione. When complex **2** was incubated with 9-ethylguanine in the presence of glutathione (γ-glutamylcysteinylglycine, GSH), a peptide believed to play an important role in driving the cellular effects of platinum drugs was formed. By using a 1:1.2:5 molar ratio, and after 24 h, a complex mixture containing as the main complex $[Pt(ppy)(1C3)(9\text{-EtG})]^+$ (3^+) was obtained, as shown by ^{1}H NMR and ESI-MS. A small peak in the mass spectra at m/z +1564.4, corresponding to a signal assignable to the dinuclear $[\{Pt(ppy)(1C3)\}_2(\mu\text{-SG})]^+$ (4^+), was also observed (Figure 11).

CONCLUSIONS

At 24 h incubation time, the new anthraquinone C,N-cycloplatinated(II) complex [Pt(ppy)Cl(1C3)] **2** was more active than cisplatin (about 9-fold) and the free ligand 1C3 (about 2-fold) in a T47D breast cancer cell line. The observation that cisplatin IC_{50} falls by about 10-fold from 24 to 72 h, whereas that for **2** changes little, suggests substantial differences in the mode of action. Complex **2** also showed high cytotoxicity against the A2780 ovarian tumor cells (about 3-fold greater than cisplatin). On the other hand, very low resistance factors (RF) of **2** in A2780*cis*R at 24−72 h (RF = 1.3) were observed. The herein reported cytotoxic compound **2** is able to interact with DNA through both intercalative and coordinative binding modes, as shown by electrophoretic mobility and UV−visible studies, with a binding constant of 5×10^3 M^{-1}. Furthermore, according to NMR and ESI-MS, the reaction of **2** with 9-ethylguanine gives the monoadduct derivative $[Pt(ppy)(1C3)(9\text{-EtG})]^+$. Theoretical calculations at the BP86/def2-TZVP level of theory on complex **2** shows a preferred extended conformation, locating the potentially intercalative amino-antraquinone moiety roughly parallel to the metal coordination plane. On the other hand, the labile Cl ligand is easily displaced by the model nucleobase 9-EtG, and the resulting adduct shows a rather weak Pt−N bond reinforced by secondary interactions that are expected to be present in the actual binding to DNA.

EXPERIMENTAL SECTION

Instrumental Measurements. The C, H, N, and S analyses were performed with a Carlo Erba model EA 1108 microanalyzer. Decomposition temperatures were determined with a SDT 2960 simultaneous DSC-TGA of TA Instruments were at a heating rate of 5 °C min^{-1}, and the solid samples were under nitrogen flow (100 mL min^{-1}). The ^{1}H, ^{13}C, and ^{195}Pt NMR spectra were recorded on a Bruker AC 300E or Bruker AV 400 spectrometer, using $SiMe_4$ and $Na_2[PtCl_6]$ as standards. ESI mass (+mode) analyses were performed on a HPLC/MS TOF 6220.

Materials. The starting complexes, $[Pt(ppy)(\mu\text{-Cl})]_2$[40] and 1C3,[22,41] were prepared by procedures described elsewhere. Solvents were dried by the usual methods. The salmon sperm DNA, sodium salt of calf thymus DNA, EDTA (ethylenediaminotetracetic acid), and Tris-HCl (tris(hydroxymethyl)-aminomethane-hydrochloride) used in the circular dichroism (CD) study were obtained from Sigma-Aldrich (Madrid, Spain); HEPES (*N*-(2-hydroxyethyl)piperazine-*N*′ ethanesulfonic acid) was obtained from ICN (Madrid, Spain), and pBR322 plasmid DNA was obtained from Boehringer-Mannheim (Mannheim, Germany).

Synthesis of [Pt(ppy)Cl(1C3)] (2). A suspension of $[Pt(ppy)(\mu\text{-Cl})]_2$ (100 mg, 0.13 mmol) in chloroform (15 mL) was stirred with **1** (73 mg, 0.26 mmol) for 48 h at room temperature to yield a solution, which was partially evaporated under vacuum; hexane was added to precipitate a red solid, which was collected by filtration and air-dried (yield: 88%). Anal. Calcd for $C_{28}H_{24}N_3ClO_2Pt$: C, 50.57; H, 3.64; N, 6.32. Found: C, 49.51; H, 3.56; N, 6.09. Mp: 187 °C (dec). ^{1}H NMR (400 MHz, $CDCl_3$): δ ($SiMe_4$) 9.66 (m, 1 H, NH), 9.30 (d, 1 H, H6

dx.doi.org/10.1021/ic101526h |*Inorg. Chem.* 2011, 50, 2151–2158

pyridyl ring of ppy, J_{H6H5} = 5 Hz, Pt satellites are observed as shoulders), 8.19 (m, 2H, 1C3), 7.72 (m, 2 H, 1C3), 7.62 (m, 1H, H4 pyridyl ring of ppy), 7.47 (d, 1H, 1C3, J = 7 Hz), 7.38 (m, 1 H, 1C3), 7.32 (d, 1 H, H3 pyridyl ring of ppy, J_{H3H4} = 8 Hz), 7.13 (dd, 1 H, H6 phenyl ring of ppy, J_{H6H5} = 7 Hz, J_{H6H4} = 1.6), 7.01 (d, 1H, 1C3, J = 8 Hz), 6.92 (m, 2H, H5 pyridyl ring of ppy and H3 phenyl ring of ppy), 6.89 (m, 2H, H5 and H4 phenyl ring of ppy), 4.37 (m, 2H, NH_2, Pt satellites are observed as shoulders), 3.56 (m, 2 H, NHCH_2), 3.34 (m, 2 H, CH_2NH_2), 2.26 (m, 2 H, CCH_2C), $^{13}C\{^1H\}$ NMR (100.8 MHz, $CDCl_3$): δ ($SiMe_4$) 150.88 (C6 pyridyl ring of ppy), 138.30 (C4 pyridyl ring of ppy), 135.25 (C 1C3), 133.94 (C 1C3), 132.99 (C 1C3), 129.97 (C5 or C4 phenyl ring of ppy), 128.92 (C3 phenyl ring of ppy or C5 pyridyl ring of ppy), 126.69 (d, 2C, C 1C3), 123.46 (C6 phenyl ring of ppy), 123.5 (C4 or C5 phenyl ring of ppy), 122.01 (C5 pyridyl ring of ppy or C3 phenyl ring of ppy), 118.07 (C3 pyridyl ring of ppy), 115.99 (C 1C3), 45.23 (CH_2NH_2), 40.01 (CH_2NH), 30.49 (C-CH_2−C), ^{195}Pt NMR [86.02 MHz, $CDCl_3$, δ]: −3374 (s). ESI^+ mass spectra (DMSO): m/z +629.2 [[Pt(ppy)(1C3)]$^+$].

Computational Details. The calculated geometries at the DFT level were fully optimized in the gas phase with tight convergence criteria using the Gaussian 09 package[42] and employing the BP86 functional, together with the extense def2-TZVP basis set on all atoms and using effective core potential (ecp) for Pt. Ultrafine grids (99 radial shells and 590 angular points per shell) were employed for numerical integrations. From these gas-phase optimized geometries, all reported data were obtained by means of single-point (SP) calculations using the B3LYP functional and the more polarized def2-TZVPP basis set. Natural charges were obtained from the natural bond orbital (NBO) population analysis. The topological analysis of the electronic charge density was conducted by means of Bader's AIM methodology using the AIM2000 software.[43] Figures 3 and 10 were generated with VMD.[44]

Biological Assays: Cell Line and Culture. The T-47D human mammary adenocarcinoma cell line used in this study was grown in RPMI-1640 medium supplemented with 10% (v/v) fetal bovine serum (FBS) and 0.2 unit/mL bovine insulin in an atmosphere of 5% CO_2 at 37 °C. The human ovarian carcinoma cell lines (A2780 and A2780*cis*R) used in this study were grown in RPMI 1640 medium supplemented with 10% (v/v) fetal bovine serum (FBS) and 2 mM L-glutamine in an atmosphere of 5% CO_2 at 37 °C.

Cytotoxicity Assay. Cell proliferation was evaluated by assay of crystal violet. T-47D cells plated in 96-well sterile plates at a density of 5 × 10^3 cells/well with 100 μL of medium and were then incubated for 48 h. After attachment to the culture surface, the cells were incubated with various concentrations of the compounds tested freshly dissolved in DMSO and diluted in the culture medium (DMSO final concentration 1%) for 24, 48, and 72 h at 37 °C. The cells were fixed by adding 10 μL of 11% glutaraldehyde. The plates were stirred for 15 min at room temperature and then washed three or four times with distilled water. The cells were stained with 100 μL of 1% crystal violet. The plates were stirred for 15 min and then washed three or four times with distilled water and dried. A total of 100 μL of 10% acetic acid was added and stirred for 15 min at room temperature. Absorbance was measured at 595 nm in a Tecan Ultra Evolution spectrophotometer.

The effects of complexes were expressed as corrected pertentage inhibition values according to the following equation

$$(\%)\ \text{inhibition} = [1 - (T/C)] \times 100$$

where T is the mean absorbance of the treated cells, and C the mean absorbance in the controls.

The inhibitory potential of compounds was measured by calculating concentration−percentage inhibition curves. These curves were adjusted to the following equation

$$E = E_{max}/[1 + (IC_{50})/C)^n]$$

were E is the percentage inhibition observed, E_{max} is the maximal effects, IC_{50} is the concentration that inhibits 50% of maximal growth, C is the concentration of compounds tested, and n is the slope of the semilogarithmic dose−response sigmoid curves. This nonlinear fitting was performed using GraphPad Prism 2.01, 1996 software (GraphPad Software, Inc.).

For comparison purposes, the cytotoxicity of cisplatin was evaluated under the same experimental conditions. All compounds were tested in two independent studies with triplicate points. The in vitro studies were performed in the USEF platform of the University of Santiago de Compostela (Spain).

Cellular Platinum Complex Accumulation. T-47D cells were plated in a 12-well cell culture plate at a density of 750000 cells/well and maintained at 37 °C in a 5% CO_2 atmosphere. Compounds to 20 μM were added to cells for either 24, 48, or 72 h, and after this time, cells were detached from the plate by using EDTA-trypsin. The cell suspension from each well was transferred to Eppendorf tubes and centrifuged at 400 *g* for 5 min at room temperature. The supernatant was discarded, and the pellet was suspended in a cell culture medium and washed by two additional centrifugations. The final pellet was resuspended in 0.5 mL of pure HNO_3 and diluted with 5 mL of Milli-Q water for ICP-MS analysis. A Varian 820-MS inductively coupled plasma-mass spectrometer was used to determine Pt concentration. Samples were introduced via a concentric glass nebulizer with a free aspiration rate of 1 mL/min, a Peltier-cooled double pass glass spray chamber, and a quartz torch. A peristaltic pump carried samples from a SPS3 autosampler (Varian) to the nebulizer. Pt standards were prepared by serial dilution of a solution containing 1000 mg/L of Pt in 5% HCl (Trace Cert. Fluka). A nine-point calibration curve was made over a concentration range of 0.2−100 μg/L Pt.

^{194}Pt was monitored, and ^{191}Ir was used as the internal standard. Data acquisition was done using peak hopping with a dwell time of 30 ms, 60 scans/replicate, and three replicates per sample from two independent experiments.

Electrophoretic Mobility Study. Fresh stocks of the water insoluble compounds were prepared by dissolving them in high purity DMSO (10^4 μM). The solution was diluted with TE buffers, with concentrations in the range of 1−10^3 μM. Appropriate dilutions were made, and the required volumes of solutions were added to the Eppendorf tubes to achieve a set of concentrations in the range of 0−100 μM. pBR322 DNA (0.7 μg) were added to each tube. The volume in each tube was adjusted to 20 μL with TE to give a final solution with a maximum 1% DMSO (v/v). The tubes were centrifuged to facilitate mixing, and the reaction was allowed to proceed by incubation at 37 °C for 24 h. A concentration range of 0−100 μM was used for the initial study of each compound, and the results of these studies were then used to select the appropriate range. A total of 4 μL of charge maker was added to 20 μL of aliquot to each tube, and the 24 μL portions were loaded on an agarose gel and electrophoretically chromatographed. The agarose gels (molecular biology certified agarose, ultra pure grade, BIO-RAD, made up to 1% w/v) were prepared using 1x TBE buffer (45 mM Tris-borate, 1 mM EDTA, pH 8.0). Electrophoresis was carried out at 55 V for 5 h. After the electrophoresis was complete, the gels were stained in TBE buffer pH 8.0 containing ethidium bromide (1 μg/mL) for 2 h. and then rinsed with water. The DNA bands were visualized with an ALPHAIMAGER EC (Alpha Innotech).

Measurement of DNA Binding Constants. UV spectroscopy was carried out on a Spectrometer UNICAM, UV 500 with operating software. The spectrophotometric titration was performed using similar conditions to those used by Kikuta et al. Salmon sperm DNA (Sigma) was dissolved in autoclaved Milli-Q H_2O and filtered (MFS 13, cellulose acetate membrane, pore 0.02 μm, Millipore). The DNA concentration was determined spectrophotometrically, ε_{260} = 6700 M^{-1} cm^{-1} (per nucleotide). Stock DNA was made to a final concentration of 560 μM (nucleobases) in HEPES buffer [10 mM, pH 8.0, with I = 0.1 ($NaNO_3$)].

Compound **2** and the ligand 1C3, 27 μM, were made in HEPES buffer [10 mM, pH 8.0, with I = 0.1 ($NaNO_3$)]. Stock DNA was added in increasing amounts (0−300 μM) to the adduct or Pt^{2+} complex or the ligand (2 mL) in a 1 cm quartz cuvette with at 25 °C. The absorption at λ_{max} was measured after each addition. The calculations for the binding constant were as described by Kikuta et al.[39] Determinations of the intrinsic binding constant, K_{app}, on the basis of the absorption titrations, may be made with the following equation

$$[DNA/\Delta\varepsilon_{app}] = [DNA]/\Delta\varepsilon + 1/K_{app}\Delta\varepsilon$$

where, $\Delta\varepsilon_{app} = \varepsilon_f - \varepsilon_A$ and $\Delta\varepsilon = \varepsilon_f - \varepsilon_B$. ε_f is the extinction coefficient for the free complex, ε_A is the extinction coefficient for the A_{obsd}/[complex], and ε_B is the extinction coefficient for the complex in the fully bound form. In plots of $[DNA]/\Delta\varepsilon_{app}$ versus [DNA], K_{app} is given by the ratio of the slope to intercept.

Two repetitions were run for each titration, and reported data are average values of both repetitions.

Reaction of the Platinum Complex 2 with 9-Ethylguanine Followed by ^{1}H NMR. The reaction was carried out in an NMR tube containing D_2O and DMSO-d_6 (1:1 in volume) as solvents. 9-Ethylguanine was incubated with complex **2** in a ratio 5:1 in the above solvents mixture at 37 °C. The concentration of complex **2** was 1.0 mM. The reaction is fast, and in less than 15 min the formation of the complex $[Pt(ppy)(1C3)(9\text{-}EtG)]^+$ ($\mathbf{3}^+$) was completed. H8 of coordinated 9-EtG was observed at δ 8.2 ppm.

Reaction of the Platinum Complex 2 with 9-Ethylguanine Followed by ESI-MS. The reaction was carried out in a vial containing H_2O and DMSO (1:1 in volume) as solvents in a similar way to that described above. ESI^+ mass spectra: m/z +808.2 $[[Pt(ppy)(1C3)(9EtG)]^+]$.

Reaction of the Platinum Complex 2 with 9-Ethylguanine in the Presence of Glutathione Followed by ESI-MS. Complex **2** (1.0 mM) was incubated in a vial containing H_2O and DMSO (1:1 in volume) as solvents, with 9-ethylguanine in the presence of glutathione GSH in a ratio 1:1.2:5, respectively. The reaction is fast, and in less than 30 min the formation mainly of $[Pt(ppy)(1C3)(9\text{-}EtG)]^+$ is observed (see above). A small peak in the mass spectra at m/z +1564.4 corresponding to a signal assignable to the dinuclear at $[\{Pt(ppy)(1C3)\}_2(\mu\text{-}SG)]^+$ ($\mathbf{4}^+$) is also observed. No important changes are observed after longer periods of time (24 h). When a similar experiment was done in the corresponding deuterated solvents, the H8 of coordinated 9-EtG was easily identified by ^{1}H NMR.

AUTHOR INFORMATION

Corresponding Author

*E-mail: jruiz@um.es; Fax: +34 868 884148; Tel: +34 868 887455.

ACKNOWLEDGMENT

This work was supported by the Ministerio de Educacion y Ciencia of Spain and FEDER (Projects CTQ2008-02178/BQU and CTQ2008-01402) and Fundación Seneca-CARM (Projects 08666/PI/08 and 04509/GERM/06).

REFERENCES

(1) Jakupec, M. A.; Galanski, M.; Arion, V. B.; Hartinger, C. G.; Keppler, B. K. *Dalton Trans.* 2008, 183–194.

(2) Jung, Y. W.; Lippard, S. J. *Chem. Rev.* 2007, *107*, 1387–1407.

(3) Kelland, L. *Nat. Rev. Cancer* 2007, *7*, 573–584.

(4) O'Dwyer, P. J., Stevenson, J. P., Johnson, S. W. In *Cisplatin. Chemistry and Biochemistry of a Leading Anticancer Drug*; Lippert, B., Ed.; Wiley-VCH: Weinheim, Germany, 1999; p 3172.

(5) Wang, D.; Lippard, S. J. *Nat. Rev. Drug Discov.* 2005, *4*, 307–320.

(6) van Zutphen, S.; Reedijk, J. *Coord. Chem. Rev.* 2005, *249*, 2845–2853.

(7) Bruijnincx, P. C. A.; Sadler, P. J. *Curr. Op. Chem. Biol.* 2008, *12*, 197–206.

(8) Bruijnincx, P. C. A.; Sadler, P. J. *Adv. Inorg. Chem.* 2009, *61*, 1–62.

(9) Lee, H. H.; Palmer, B. D.; Baguley, B. C.; Chin, M.; McFadyen, W. D.; Wickham, G.; Thorsbournepalmer, D.; Wakelin, L. P. G.; Denny, W. A. *J. Med. Chem.* 1992, *35*, 2983–2987.

(10) Temple, M.; McFadyen, W. D.; Holmes, R. J.; Denny, W. A.; Murray, V. *Biochemistry* 2000, *39*, 5593–5599.

(11) Perrin, L. C.; Prenzler, P. D.; Cullinane, C.; Phillips, D. R.; Denny, W. A.; McFadyen, W. D. *J. Inorg. Biochem.* 2000, *81*, 111–117.

(12) Bowler, B. E.; Ahmed, K. J.; Sundquist, W. I.; Hollis, L. S.; Whang, E. E.; Lippard, S. J. *J. Am. Chem. Soc.* 1989, *111*, 1299–1306.

(13) Sundquist, W. I.; Bancroft, D. P.; Lippard, S. J. *J. Am. Chem. Soc.* 1990, *112*, 1590–1596.

(14) Gean, K. F.; Ben-Shoshan, R.; Ramu, A.; Ringel, I.; Katzhendler, J; Gibson, D. *Eur. J. Med. Chem.* 1991, *26*, 593–598.

(15) Gibson, D.; Gean, K. F.; Ben-Shoshan, R.; Ramu, A.; Ringel, I.; Katzhendler, J. *J. Med. Chem.* 1991, *34*, 414–420.

(16) Gibson, D.; Mansur, N.; Gean, K. F. *J. Inorg. Biochem.* 1995, *58*, 79–88.

(17) Gibson, D.; Binyamin, I.; Haj, M.; Ringel, I.; Ramu, A; Katzhendler, J. *Eur. J. Med. Chem.* 1997, *32*, 823–831.

(18) Kalayda, G. V.; Jansen, B. A.; Molenaar, C; Wielaard, P.; Tanke, H. J.; Reedijk, J. *J. Biol. Inorg. Chem.* 2004, *9*, 414–22.

(19) Kalayda, G. V.; Jansen, B. A.; Wielaard, P.; Tanke, H. J.; Reedijk, J. *J. Biol. Inorg. Chem.* 2005, *10*, 305–15.

(20) Baruah, H.; Barry, C. G.; Bierbach, U. *Curr. Top. Med. Chem.* 2004, *4*, 1537–1549.

(21) Guddneppanavar, R.; Choudhury, J. R.; Kheradi, A. R.; Steen, B. D.; Saluta, G.; Kucera, G. L.; Day, C. S.; Bierbach, U. *J. Med. Chem.* 2007, *50*, 2259–2263.

(22) Alderden, R. A.; Mellor, H. R.; Modok, S.; Hambley, T. W.; Callaghan, R. *Biochem. Pharmacol.* 2006, *71*, 1136–1145.

(23) Whan, R. M.; Messerle, B. A.; Hambley, T. W. *Dalton Trans.* 2009, 932–939.

(24) Bryce, N. S.; Zhang, J. Z.; Whan, R. M.; Yamamoto, N.; Hambley, T. W. *Chem. Commun.* 2009, 2673–2675.

(25) Klein, A. V.; Hambley, T. W *Chem. Rev.* 2009, *109*, 4911–4920.

(26) Ruiz, J.; Lorenzo, J.; Vicente, C.; López, G.; López-De-Luzuriaga, J. M.; Monge, M.; Avilés, F. X.; Bautista, D.; Moreno, V.; Laguna, A. *Inorg. Chem.* 2008, *47*, 6990–7001.

(27) Ruiz, J.; Rodríguez, V.; Cutillas, N.; López, G.; Bautista, D. *Inorg. Chem.* 2008, *47*, 10025–10036.

(28) Ruiz, J.; Rodríguez, V.; de Haro, C.; Espinosa, A.; Pérez, J.; Janiak, C. *Dalton. Trans.* 2010, *39*, 3290–3301.

(29) Bader, R. F. W. *Atoms in Molecules: A Quantum Theory*; Oxford University Press: Oxford, 1990.

(30) Loh, S. Y.; Mistry, P.; Kelland, L. R.; Abel, G.; Harrap, K. R. *Br. J. Cancer* 1992, *66*, 1109–1115.

(31) Goddard, P. M; Orr, R. M.; Valenti, M. R.; Barnard, C. F.; Murrer, B. A.; Kelland, L. R.; Harrap, K. R. *Anticancer Res.* 1996, *16*, 33–38.

(32) Behrens, B. C.; Hamilton, T. C.; Masuda, H.; Grotzinger, K. R.; Whang-Peng, J.; Louie, K. G.; Knutsen, T.; McKoy, W. M.; Young, R. C.; Ozols, R. F. *Cancer Res.* 1987, *47*, 414–418.

(33) Kelland, L. R.; Barnard, C. F. J.; Mellish, K. J.; Jones, M.; Goddard, P. M.; Valenti, M.; Bryant, A.; Murrer, B. A.; Harrap, K. R. *Cancer Res.* 1994, *54*, 5618–5622.

(34) Ghezzi, A. R.; Aceto, M.; Casino, C.; Gabano, E.; Osella, D. *J. Inorg. Biochem.* 2004, *98*, 73–78.

(35) Janovska, E.; Novakova, O.; Natile, G.; Brabec, V *J. Inorg. Biochem.* 2002, *90*, 155–158.

(36) Ellis, L. T.; Perkins, D. F.; Turner, P.; Hambley, T. W. *Dalton. Trans.* 2003, 2728–2736.

(37) Kikuta, E.; Matsubara, R.; Katsube, N.; Koike, T.; Kimura, E. *J. Inorg. Biochem.* 2000, *82*, 239–249.

(38) Pt-C(ppy) d_{Pt-C} = 1.995 Å, $\rho(\mathbf{r}_c) = 15.89 \times 10^{-2}$ e/a_o^3; Pt-N(ppy) d_{Pt-N} = 2.041 Å, $\rho(\mathbf{r}_c) = 12.24 \times 10^{-2}$ e/a_o^3; and Pt-N(1C3) d_{Pt-N} = 2.081 Å, $\rho(\mathbf{r}_c) = 11.37 \times 10^{-2}$ e/a_o^3.

(39) Hydrogen bonding between the 9-EtG carbonyl group and a 1C3 NH group ($d_{CO\cdots HN}$ = 1.848 Å; $\rho(\mathbf{r}_c) = 3.39 \times 10^{-2}$ e/a_o^3) and p-stacking type interaction between a pyridine C-H atom and the 9-EtG ring system (closest ring atom C8: $d_{CH\cdots C8}$ = 2.577 Å; $\rho(\mathbf{r}_c) = 1.02 \times 10^{-2}$ e/a_o^3).

(40) Chang, S. Y.; Cheng, Y.-M.; Chi, Y.; Lin, Y.-C.; Jiang, C. M.; Lee, G. H.; Chou, P.-T. *Dalton Trans.* 2008, 6901–6911.

(41) Gibson, D.; Binyamin, I; Haj, M.; Ringel, I.; Ramu, A.; Katzhendler, J. *Eur. J. Med. Chem.* 1997, *32*, 823–831.

(42) Gaussian 09, Revision A.2; Frisch, M. J.; Trucks, G. W.; Schlegel, H. B.; Scuseria, G. E.; Robb, M. A.; Cheeseman, J. R.; Scalmani, G.; Barone, V.; Mennucci, B.; Petersson, G. A.; Nakatsuji, H.; Caricato, M.; Li, X.; Hratchian, H. P.; Izmaylov, A. F.; Bloino, J.; Zheng, G.; Sonnenberg, J. L.; Hada, M.; Ehara, M.; Toyota, K.; Fukuda, R.; Hasegawa, J.; Ishida, M.; Nakajima, T.; Honda, Y.; Kitao, O.; Nakai, H.; Vreven, T.; Montgomery, Jr., J. A.; Peralta, J. E.; Ogliaro, F.; Bearpark, M.; Heyd, J. J.; Brothers, E.; Kudin, K. N.; Staroverov, V. N.; Kobayashi, R.; Normand, J.; Raghavachari, K.; Rendell, A.; Burant, J. C.; Iyengar, S. S.; Tomasi, J.; Cossi, M.; Rega, N.; Millam, N. J.; Klene, M.; Knox, J. E.; Cross, J. B.; Bakken, V.; Adamo, C.; Jaramillo, J.; Gomperts, R.; Stratmann, R. E.; Yazyev, O.; Austin, A. J.; Cammi, R.; Pomelli, C.; Ochterski, J. W.; Martin, R. L.; Morokuma, K.; Zakrzewski, V. G.; Voth, G. A.; Salvador, P.; Dannenberg, J. J.; Dapprich, S.; Daniels, A. D.; Farkas, Ö.; Foresman, J. B.; Ortiz, J. V.; Cioslowski, J.; Fox, D. J. Gaussian, Inc.: Wallingford, CT, 2009.

(43) (a) AIM2000, v. 2.0; Biegler-König, F. W.; Schönbohm, J. 2002. http://www.aim2000.de/.(b) Biegler-König, F.; Schönbohm, J.; Bayles, D. J. *Comp. Chem.* 2001, *22*, 545–559. (c) Biegler-König, F.; Schönbohm, J. *J. Comput. Chem.* 2002, *23*, 1489–1494.

(44) VMD, Visual Molecular Dynamics; Humphrey, W.; Dalke, A.; Schulten, K. *J. Molec. Graphics*, **1996**, *14*, 33−38. http://www.ks.uiuc.edu/Research/vmd/.